



### RESEARCH ARTICLE

### OPEN ACCESS

## IMPROVEMENT IN POWER CONTROL OF DOUBLY FED INDUCTION GENERATOR USING AN INTERVAL TYPE-2 FUZZY LOGIC CONTROLLER

Izzeddine Allali <sup>1</sup>, Abdelber Bendaoud <sup>2</sup>

<sup>1</sup>IRECOM Laboratory, Faculty of Electrical Engineering, Djilali Liabès University of Sidi Bel-Abbès, BP 89 Sidi Bel Abbès 22000, Algeria.

<sup>2</sup>APELEC Laboratory, Faculty of Electrical Engineering, Djilali Liabès University of Sidi Bel-Abbès, BP 89 Sidi Bel Abbès 22000, Algeria

<sup>1</sup><http://orcid.org/0009-0006-3668-7336>, <sup>2</sup><http://orcid.org/0000-0002-4502-4415>

Email: [izzeddine.allali@univ-sba.dz](mailto:izzeddine.allali@univ-sba.dz), [abdelber.bendaoud@univ-sba.dz](mailto:abdelber.bendaoud@univ-sba.dz).

### ARTICLE INFO

#### Article History

Received: September 6, 2025.

Revised: October 20, 2025.

Accepted: November 1, 2025.

Published: November 30, 2025.

#### Keywords:

Doubly fed induction generator, wind power, interval type-2 fuzzy logic control, type-1 fuzzy logic control.

### ABSTRACT

This article presents two advanced fuzzy logic control algorithms—Type 1 (T1-FLC) and Interval Type 2 (IT2-FLC)—applied to regulate a doubly fed induction generator (DFIG) for a wind energy conversion system (WECS). These nonlinear control methodologies are effective in addressing model uncertainties. Although T1-FLCs perform adequately in many scientific and engineering applications, their efficacy diminishes under conditions of significant uncertainty arising from parameter variations, abrupt speed changes, or external disturbances. Conversely, IT2-FLCs constitute a more recent class of intelligent controllers explicitly designed to enhance robustness against such uncertainties and unreliable information. The proposed control strategy incorporates a dual-loop structure, featuring an inner loop for rotor current regulation and an outer loop for stator power control. Simulation results under diverse speed and parameter variations confirm that IT2-FLC exhibits superior robustness, faster response times, reduced overshoot, and achieves a 26.22% and 77.82% reduction in current total harmonic distortion (THD) compared to the T1-FLC approach.



Copyright ©2025 by authors and Galileo Institute of Technology and Education of the Amazon (ITEGAM). This work is licensed under the Creative Commons Attribution International License (CC BY 4.0).

## I. INTRODUCTION

Energy is vital for infrastructure, economic growth, and global welfare. Rising fossil fuel use pushes engineers toward eco-friendly renewable [1-3]. Traditional fuels emit harmful gases that damage health and cause global warming, leading to ice melt and rising temperatures. These fuels are depleting, and import dependence creates global reliance. Thus, governments invest in affordable, clean, simple, and readily available energy solutions without extra infrastructure. Natural sources like solar, wind, geothermal, and hydro effectively tackle environmental challenges, reduce electricity costs, and lessen dependence on external supplies. Known as renewable sources, they are widely used due to their availability year-round and ease of use, requiring no advanced technology [4]. WECS are among the most established green energy solutions, with total global capacity expected to reach nearly 1 terawatt of additional installations by 2030. Wind turbines (WT) are key components of electrical power systems and remain the focus of research dedicated to enhancing the quality and output of electricity generated from wind energy (WE) [5].

At present, the majority of WTs utilize doubly-fed induction generators (DFIG) owing to their benefits, which include variable speed operation, independent control of active and reactive power ( $P_s$  and  $Q_s$ ), diminished mechanical stress and noise, enhanced power quality, lower costs, and greater durability [6]. Conventional proportional-integral (PI) controllers are used to regulate DFIGs but often suffer from errors and reduced accuracy under varying wind speeds (WS), nonlinear conditions, and internal factors like temperature and magnetic saturation [7], [8]. Hence, a more robust control method is needed to optimize DFIG performance and improve power quality. This can be achieved by modeling the nonlinear process with fuzzy logic, a methodology grounded in fuzzy set theory first proposed by Lotfi Zadeh in 1965. Fuzzy logic excels at handling imprecise information and finds applications in expert systems, data classification, signal processing, database management, modeling, and automatic control. Its first control application was Mamdani's 1974 steam engine project, followed by industrial use in controlling a cement kiln with linguistic if-then rules in Mamdani's fuzzy inference system. [9], [10]. Researchers initially focused on type 1 fuzzy logic controllers (T1-FLC), which feature precisely defined two-dimensional

membership functions (MFs). However, as new and more complex challenges arose, the focus shifted to type 2 fuzzy logic controllers (T2-FLC), which use three-dimensional MFs. The additional dimension facilitates the representation of uncertainties inherent in linguistic terms, especially when the shape or parameters of MFs are not specified. Thus, type 2 fuzzy sets provide an effective mechanism for managing linguistic uncertainties through the use of type 2 MFs [11]. Although type 2 fuzzy sets are computationally complex and more difficult to implement, their utilization is justified due to their efficacy in scenarios characterized by significant uncertainty in MF determination, as well as their capability to mitigate uncertainty and non-linearity [11], [12]. To reduce the computational burden, an interval type 2 fuzzy logic system (IT2-FLS) has been addressed. Therefore, IT2-FLS are widely preferred over general type 2 fuzzy logic systems [11]. T2-FLS utilize the uncertainty footprint (FOU) to address these challenges with great efficiency. Empirical evidence demonstrates that T2-FLS significantly outperforms T1-FLS in these areas [13], [14]. The fuzzy logic controller (FLC) that is being discussed here is well-known for producing improved results for non-linear systems that have changing parameters.

The DFIG is therefore a great choice for evaluating the efficiency of FLCs because of this. Many previous studies have applied IT2-FLC dedicated to controlling DFIG-Based WECS in the literature, such as in [15], where the authors developed an IT2-FLC algorithm to enhance the control of Ps and Qs. Simulation results demonstrated satisfactory control performance and improved power conversion in wind systems. In [16], IT2-FLC-tuned PI controllers were employed to achieve optimal torque control for WTs driven by DFIGs. This control strategy effectively regulates mechanical rotor speed error, enhancing overall system performance. In [17], an IT2-FLC controller was designed for the nonlinear modeling of turbine blades and subsequently integrated into a comprehensive DFIG wind turbine model, with an additional IT2-FLC applied to regulate rotor frequency and voltage amplitude. The work in [18] introduced an adaptive sliding mode type-2 neuro-fuzzy controller to manage DFIG power output, resulting in improved performance and heightened system robustness. In [19], both T1-FLC and T2-FLC methods were investigated under direct and indirect control modes, with a comprehensive evaluation of their performance. The study identified the most effective control method in terms of reference tracking and robustness.

In [14], an IT2-Fuzzy Sliding Mode Controller (IT2-FSMC) was proposed for DFIG management in WECS by integrating sliding mode control with FL principles. Comparative analyses underscore that IT2-FSMC methods outperform T1-FSMC approaches, delivering superior control effectiveness and enhanced outcomes. Unlike previous research, this paper proposes an innovative approach that includes the IT2-FLC strategy for separate control of the Ps and Qs of the stator. This system consists of two control loops: an inner loop for regulating the rotor current and an outer loop for controlling the stator power. The contribution of this research lies in the use of the IT2-FLC strategy to control the power of grid-connected DFIGs to reduce ripples, improve power quality, and increase system robustness. This paper also includes a comprehensive and detailed comparison with the T1-FLC methodology. The proposed techniques were tested according to the following criteria: setpoint tracking under varying WS, sensitivity to parameter variations to assess robustness, and harmonic analysis to determine the controller's effectiveness in mitigating distortion. Overall, these evaluations demonstrate the proposed scheme's capability to improve DFIG dynamic behavior and power quality.

The following are the study's primary goals:

- Increase the robustness of IT2-FLC control.
- Reduce THD of current using IT2-FLC.
- Demonstrate that IT2-FLC provides superior improvements in power quality compared to the T1-FLC approach.
- Minimize overshoot and improve dynamic response.

## II. MATERIALS AND METHODS

### II.1 MODELING THE CONVERSION SYSTEM

Figure 1 clearly shows the components and layout of the WECS.

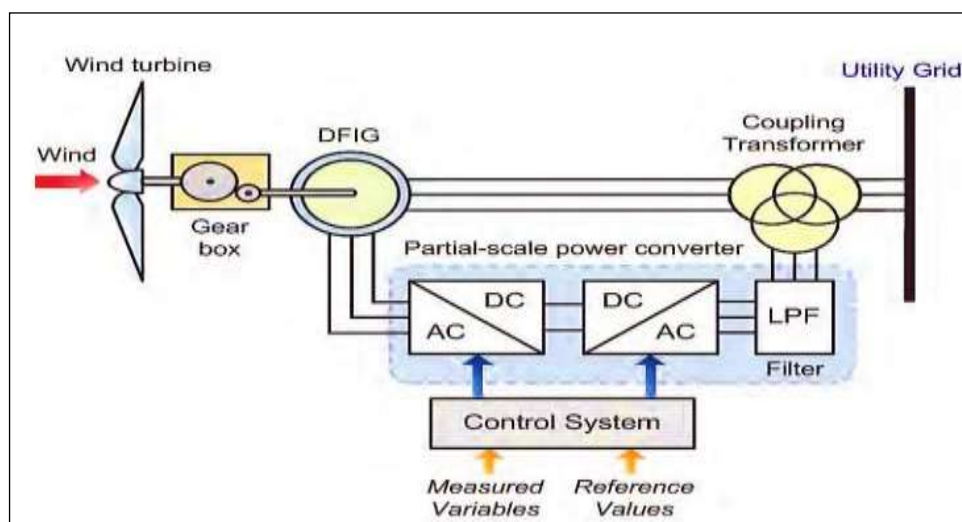


Figure 1: WT structure based on DFIG.

Source: [20].

### II.1.1 MODELING THE TURBINE

A WT converts the kinetic energy of wind moving at speed  $V$  across the surface area  $S$  of its three blades, each with length  $R_t$ , into mechanical energy. The power coefficient  $C_p(\lambda, \beta)$  is the ratio of the WT's kinetic energy that can be extracted and converted into mechanical energy. This coefficient varies according to the turbine's design. WTs can be represented mathematically using the following equations [21-23]:

$$P_m = \frac{1}{2} \rho \pi R^2 v^3 C_p \quad (1)$$

$$\lambda = \frac{\Omega R}{v} \quad (2)$$

$$C_p(\lambda, \beta) = (0.5 - 0.00167(\beta - 2)) \sin \left[ \frac{\pi(\lambda + 0.1)}{18.5 - 0.3(\beta - 2)} \right] - 0.00184(\lambda - 3)(\beta - 2) \quad (3)$$

Based on the power output of the WT and knowing the turbine's rotational speed, the mechanical torque is expressed as follows [22], [23]:

$$T_m = \frac{P_m}{\Omega} = \frac{1}{2\lambda} \rho \pi R^3 v^2 C_p \quad (4)$$

In order to improve the performance of the WT, the maximum power point tracking (MPPT) control system has to accurately manage the rotational speed while simultaneously ensuring that the blade pitch angle ( $\beta$ ) consistently remains at its minimum value. This particular technique guarantees that the power coefficient ( $C_p$ ) is maximized at the ideal tip speed ratio ( $\lambda_{opt}$ ), hence obtaining the  $C_{p-max}$ , as stated in references [11, 13]. Additionally, the torque reference  $T_{m-ref}$  was defined by [24], [25].

$$T_{m-ref} = \frac{\rho C_{p-max}}{2} \frac{R_t^5}{\lambda_{opt}^3} \frac{\Omega_{mec}^2}{G} \quad (5)$$

The control device allows all blades to be rotated at an equal angle or independently. This independent adjustment provides greater freedom for the control system. This special process reduces the stress on the blades. It monitors the energy generated by the WT to achieve optimal performance at every WS [26].

### II.1.2 MODELING OF THE DFIG

The control of DFIG presents considerable challenges due to their inherently complex, nonlinear dynamics. Effective management of such machines necessitates the development of an accurate model that faithfully replicates their actual behavior. The electrical equations governing the DFIG are provided and have been reformulated within the Park reference frame, as illustrated in equations (6) and (7). [27,28].

$$\begin{cases} V_{sd} = R_s I_{sd} + \frac{d\phi_{sd}}{dt} - \omega_s \phi_{sq} \\ V_{sq} = R_s I_{sq} + \frac{d\phi_{sq}}{dt} + (\omega_s - \omega_r) \phi_{sd} \\ V_{rd} = R_r I_{rd} + \frac{d\phi_{rd}}{dt} - \omega_s \phi_{rq} \\ V_{rq} = R_r I_{rq} + \frac{d\phi_{rq}}{dt} + (\omega_s - \omega_r) \phi_{rd} \end{cases} \quad (6)$$

With:

$$\begin{cases} \phi_{sd} = L_s I_{sd} + M I_{rd} \\ \phi_{sq} = L_s I_{sq} + M I_{rq} \\ \phi_{rd} = L_r I_{rd} + M I_{sd} \\ \phi_{rq} = L_r I_{rq} + M I_{sq} \end{cases} \quad (7)$$

The following equation governs the mechanical equation:

$$\Gamma_{em} = \Gamma_r + C_f \Omega_{mec} + J_T \frac{d\Omega_{mec}}{dt} \quad (8)$$

The electromagnetic torque is given by the following equation:

$$\Gamma_{em} = p \frac{M}{L_s} (\phi_{sd} I_{rq} - \phi_{sq} I_{rd}) \quad (9)$$

The definitions pertaining to DFIG power are as follows:

$$\begin{cases} P_s = V_{sd} I_{sd} + V_{sq} I_{sq} \\ Q_s = V_{sq} I_{sd} - V_{sd} I_{sq} \end{cases} \quad (10)$$

To regulate wind power generation effectively, one method involves decoupling the control of  $P_s$  and  $Q_s$  by linking the voltages generated by an inverter to the stator power. To enhance the control of the DFIG, independent control of  $P_s$  and  $Q_s$  will be implemented through the orientation of the stator flux. The goal is to align the stator flux within a rotating reference frame. For medium-power machines utilized in WECS, the stator resistance  $R_s$  is considered negligible; thus, the electrical equations governing the DFIG model are expressed as follows [29]:

$$\Phi_{sd} = \phi_s \quad \text{et} \quad \phi_{sq} = 0 \tag{11}$$

The flux equation (7) can be written as shown below:

$$\begin{cases} \phi_{sd} = L_s I_{sd} + M I_{rd} \\ 0 = L_s I_{sq} + M I_{rq} \end{cases} \tag{12}$$

The stator voltage equations can also be expressed more simply as shown below.

$$V_{sd} = 0, \quad V_{sq} = V_s = \omega_s \phi_s \tag{13}$$

Using equation (12), it is possible to establish a relationship between the stator and rotor currents.

$$\begin{cases} I_{sd} = -\frac{M}{L_s} I_{rd} + \frac{\phi_s}{L_s} \\ I_{sq} = -\frac{M}{L_s} I_{rq} \end{cases} \tag{14}$$

By replacing the terms  $I_{sd}$  and  $I_{sq}$  with their expressions from equation (14) and setting  $V_{sd} = 0$ , the Ps and Qs of the stator can be written as follows:

$$\begin{cases} P_s = V_s I_{sq} = -V_s \frac{M}{L_s} I_{rq} \\ Q_s = V_s I_{sd} = -V_s \frac{M}{L_s} I_{rd} + V_s \frac{\phi_s}{L_s} \end{cases} \tag{15}$$

We then establish the equations that relate the rotor voltages to the rotor currents.

$$\begin{cases} V_{rd} = R_r I_{rd} + \left(L_r - \frac{M^2}{L_s}\right) \frac{dI_{rd}}{dt} - g \omega_s \left(L_r - \frac{M^2}{L_s}\right) I_{rq} \\ V_{rq} = R_r I_{rq} + \left(L_r - \frac{M^2}{L_s}\right) \frac{dI_{rq}}{dt} + g \omega_s \left(L_r - \frac{M^2}{L_s}\right) I_{rd} + g \frac{M V_s}{L_s} \end{cases} \tag{16}$$

## II.2 FUZZY LOGIC CONTROL

Type 2 fuzzy logic is widely utilized, particularly in its control unit, which is esteemed for its robust disturbance management and enhanced performance under conditions of random noise. The distinctions between Type 1 and Type 2 FL are as follows[30]:

- The MF is two-dimensional in Type 1, whereas it is three-dimensional in Type 2;
- The membership value is precise in Type 1 but exhibits fuzziness in Type 2;
- Additionally, Type 2 incorporates an uncertainty footprint that provides an extra degree of freedom, a feature absent in Type 1.

A T2-FLC fundamentally builds upon established concepts similar to those employed in a T1-FLC, including MFs, rule bases, t-norm operations, fuzzification, inference, and defuzzification [31]. Nevertheless, the altered characteristics of MFs within a higher-type framework necessitate modifications to the operational processes during inference. The core principles of FL remain invariant regardless of MF structure and thus are preserved. Consequently, a T2FLS exhibits substantial methodological congruence with a T1FLS. The principal distinction resides within the system's third component, where output processing encompasses not only defuzzification but also the type reduction stage. This addition is essential due to the inherent complexity introduced by the more intricate MF representations, which require type reduction before defuzzification. The architecture of a T2FLS is depicted in Figure 2.

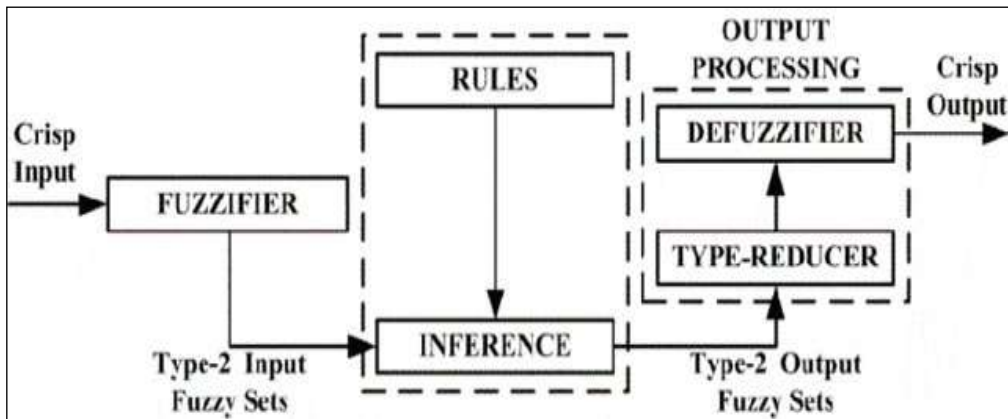


Figure 2: IT2- FLS configuration.

Source: [32].

### II.2.1 CONTROL OF DFIG USING IT2-FLC

Figure 3 depicts a schematic of the system being considered, with the two control loops for power and current shown clearly on each axis. Additionally, traditional T1-FLC and IT2-FLC controllers are both assessed.

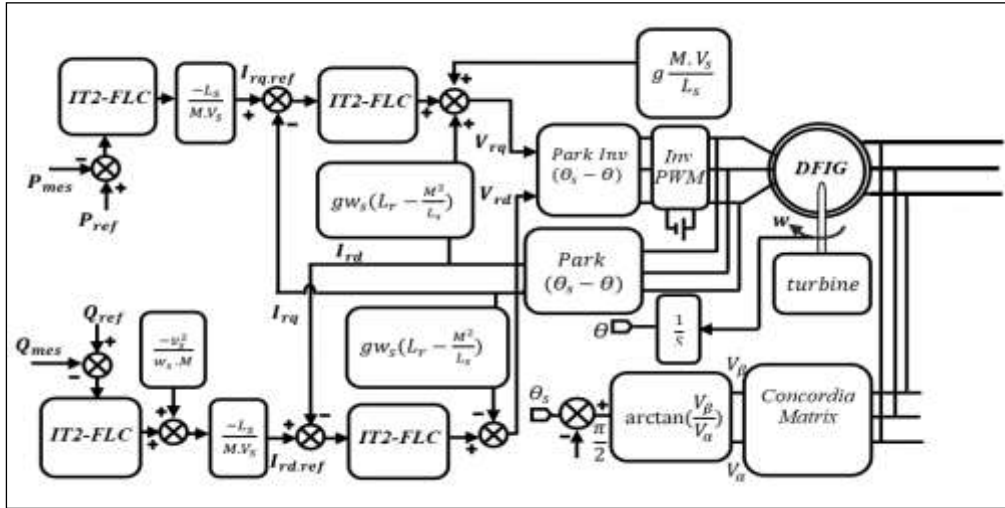


Figure 3: Control of the IT2-FLC.  
Source: Authors, (2025).

### II.2.2 STRUCTURE OF IT2-FLC

Figure 4 presents the block diagram of an IT2-FLC, which is developed based on a T1-FLC. The normalized variables, referred to as norms, play a crucial role in adjusting the gains at both the controller's input and output to achieve the desired system response. In IT2-FLS that consists of a total of  $M$  rules, the specific rule identified as the  $i^{\text{th}}$  rule is expressed or formulated in the following manner:

$$R^i: \text{if } e \text{ is } \tilde{F}_e^i \text{ and } de \text{ is } \tilde{F}_{de}^i \text{ then } dl_r^{\text{ref}} \text{ is } \tilde{G}^i ; i=1, \dots, M \quad (17)$$

$\tilde{F}_e^i$  and  $\tilde{F}_{de}^i$  denote the linguistic terms associated with the inputs ( $e$ ,  $de$ ), while  $\tilde{G}^i$  signifies the linguistic term corresponding to the output  $dl_r^{\text{ref}}$ . The output's linguistic terms are defined by their type-1 interval MF, represented as  $[u_1^i, u_2^i]$ . These functions are obtained by calculating the centroid of the T2-FS associated with the output.

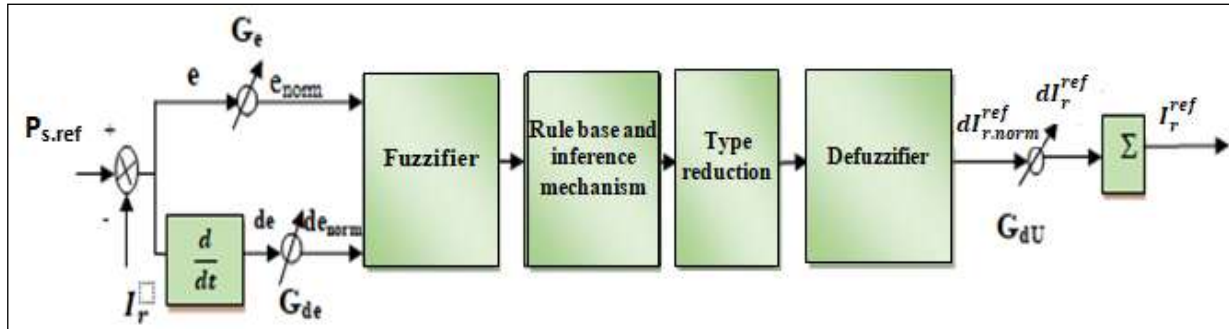


Figure 4: Structure of an IT2-FLC.  
Source: Authors, (2025).

Figure 5 depicts the MFs associated with both the antecedent and consequent components. The domains for the input and output variables are normalized and confined to the range  $[-1, 1]$ .

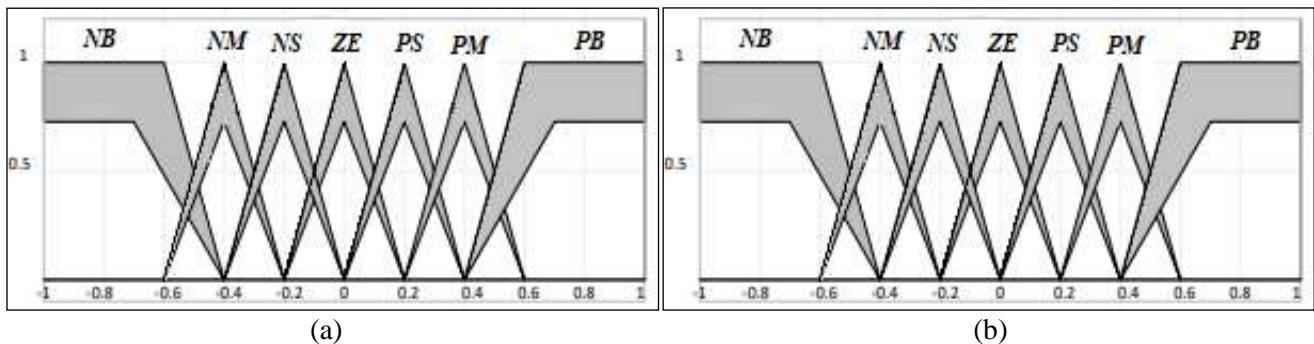


Figure 5: Type 2 fuzzy MFs of the variation of: (a)  $e$  and  $de$ , (b)  $output$ .  
Source: Authors, (2025).

The set of  $M$  rules described above may be expressed through an inference matrix. As illustrated in Table 1, the fuzzy rules that govern the controller used in this research are presented in that format.

Table 1: Table of rules for the T-2 FLC.

<i>ede</i>	NB	NM	NS	ZE	PS	PM	PB
NB	NB	NB	NB	NB	NM	NS	ZE
NM	NB	NB	NB	NM	NS	ZE	PS
NS	NB	NB	NM	NS	ZE	PS	PM
ZE	NB	NM	NS	ZE	PS	PM	PB
PS	NM	NS	ZE	PS	PM	PB	PB
PM	NS	ZE	PS	PM	PB	PB	PB
PB	ZE	PS	PM	PB	PB	PB	PB

Source: Authors, (2025).

### III. SIMULATION RESULTS

This simulation section uses a 10 kW generator that is connected to a 400 V, 50 Hz electrical grid. The system parameters are provided in the Appendix. To evaluate the performance of the controllers, two controllers (T1-FLC and IT2-FLC) were compared using two tests. The first tests assessed tracking, while the second tests involved a robust assessment of variations in machine parameters.

#### III.1 FIRST TEST

The strategies that have been presented for regulating the performance of the generator under ideal circumstances are validated in this part. This section assumes that there are no operational disruptions and that there are no adjustments to the machine parameters. The wind profile illustrated in Figure 0.6 shows that the WT will experience an average speed of approximately 10 m/s. The derived power is notably influenced by even a slight change in WS, as it is directly proportional to the cube of the WS. The diagram clearly indicates that the  $P_s$  displayed a negative sign, which signifies that the DFIG produced and supplied energy to the grid. The reactive power control function enables the adjustment of  $Q_s$  to exhibit either negative values, indicating inductive behavior, or positive values, indicating capacitive behavior. Setting the  $Q_s$  response to zero within the time frame of 0 to 2 seconds facilitates operation at a unity power factor, as demonstrated in Figure 07(b). The performance attained with the T1FLC and IT2FLC controls is commendable, as evidenced by the trajectory tracking and the swift convergence of the measured variables to the target reference, as depicted in Figure 07. The application of this methodology enabled a precise decoupling of the two components of the stator power.

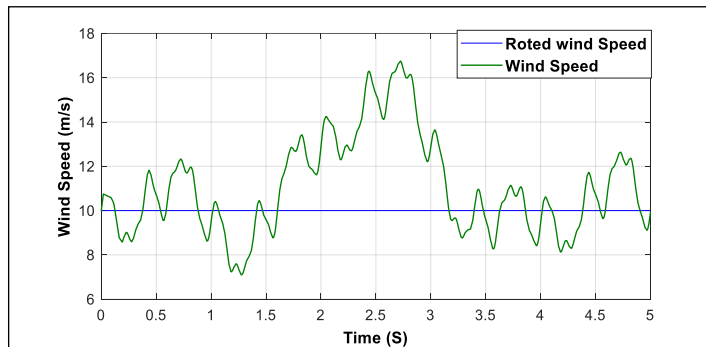


Figure 6: WS profile.  
Source: Authors, (2025).

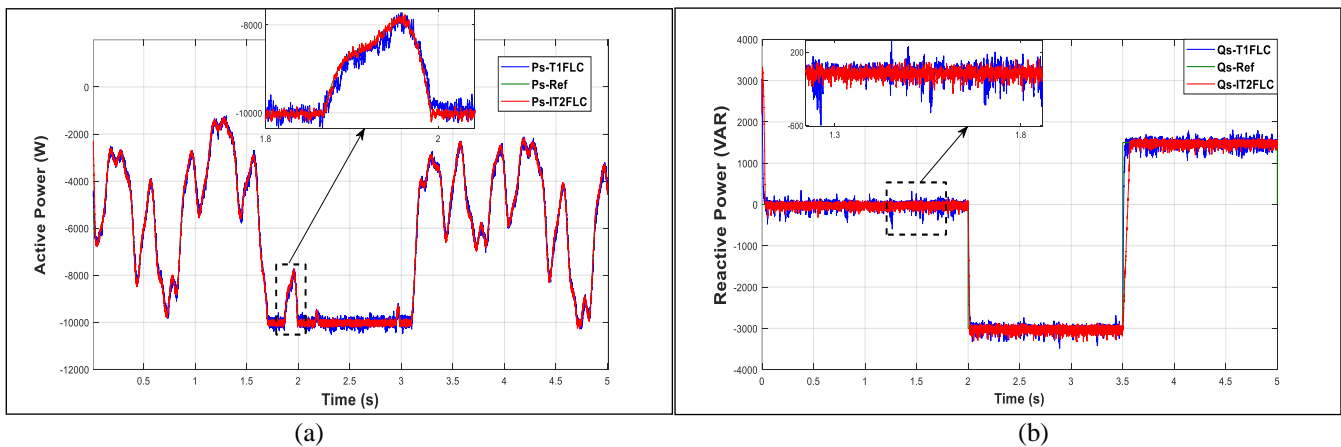


Figure 7: DFIG power (a)  $P_s$ ; (b)  $Q_s$ .  
Source: Authors, (2025).

Figure 8 presents the d- and q-axis components of the rotor current, which relate respectively to the stator's  $P_s$  and  $Q_s$ . The rotor currents tracked their reference profiles accurately, and no overshoot was observed.

Figure 9(a) illustrates the stator currents as sinusoidal signals at 50 Hz, with amplitudes that change according to WS. In contrast, Figure 9(b) depicts the rotor-circuit currents also as sinusoidal waveforms whose frequency and amplitude vary in response to slip or generator rotational speed. Figure 10 shows the pulse-modulated output voltages produced by the rotor-side converter. These voltages change in form with variations in generator speed and with adjustments to the rotor voltage reference magnitude.

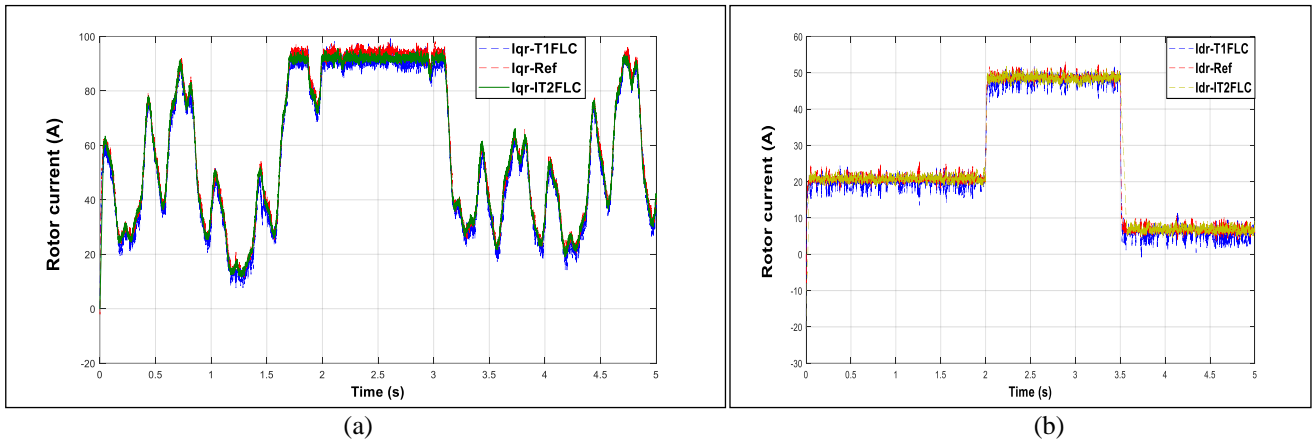


Figure 08: rotor current (a) ; (b)  $I_{dr}$ .  
Source: Authors, (2025).

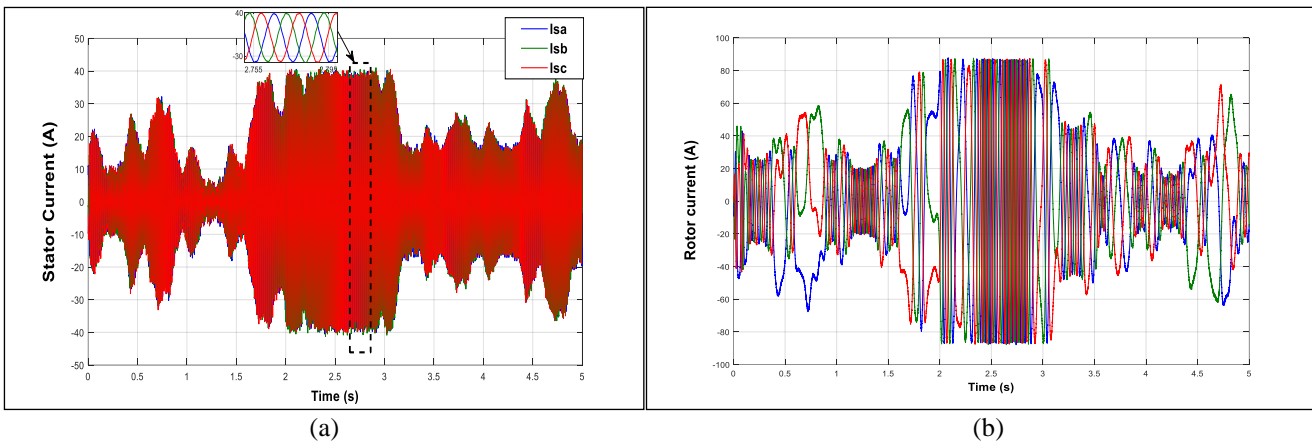


Figure 9: (a) stator current ; (b) rotor current.  
Source: Authors, (2025).

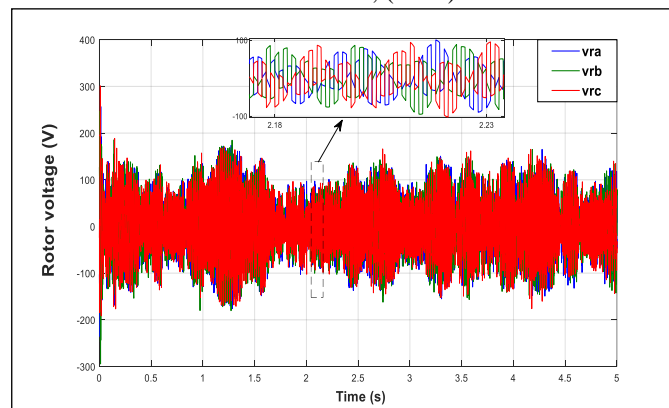


Figure 10: Rotor voltage.  
Source: Authors, (2025).

Figure 11 presents the single-phase stator current harmonic spectrum of the DFIG, obtained via the Fast Fourier Transform (FFT) technique for both control schemes. A comparison of the results reveals a clear reduction in total harmonic distortion when using the proposed IT2-FLC: the THD drops from 1.83% under the T1-FLC to 1.35% with the IT2-FLC. This represents an approximate 26.22% improvement in harmonic performance, demonstrating that the IT2-FLC approach provides superior energy quality relative to the conventional T1-FLC. Furthermore, the IT2-FLC produces a higher basic signal amplitude at 50 Hz than the T1-FLC, which reinforces the conclusion that the proposed controller outperforms the traditional design in terms of both harmonic suppression and fundamental amplitude.

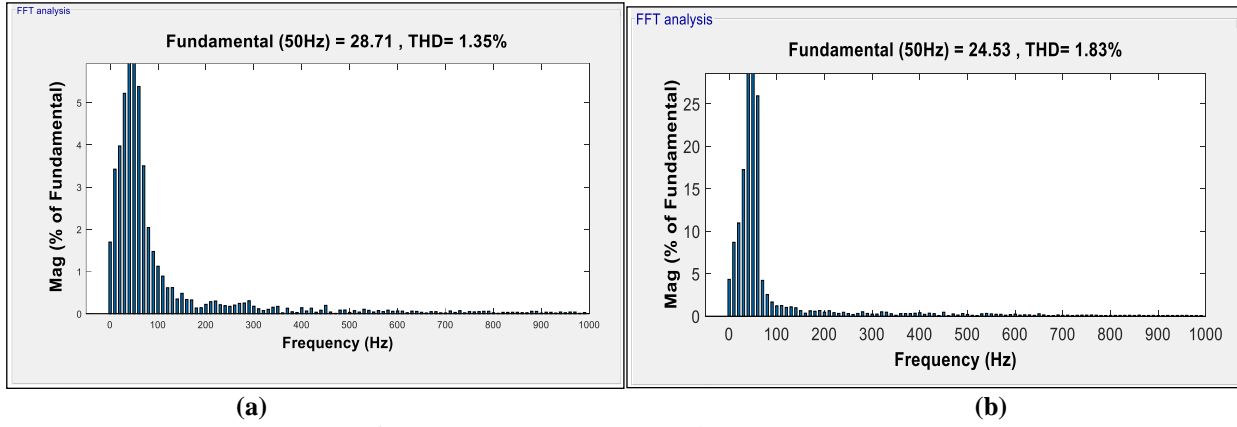


Figure 11: (a) THD IT2-FLC; (b) THD T1-FLC. Source: Authors, (2025).

### III.2 ROBUSTNESS TEST

This section assesses the resilience and performance of the proposed controllers when subjected to unfavorable variations in system parameters. Both graphical and quantitative results are presented and contrasted with those obtained using a traditional control strategy. The robustness assessment entails deliberate alterations to the generator’s internal parameters to examine how well the proposed unit withstands uncertainties and how rapidly it responds relative to the conventional controller. Specifically, the stator and rotor resistances ( $R_s, R_r$ ) are doubled, while the stator and rotor inductances ( $L_s, L_r$ ) were reduced to 30% of their original magnitudes. Additionally, the mutual inductance  $M$  was decreased to half of its initial value.

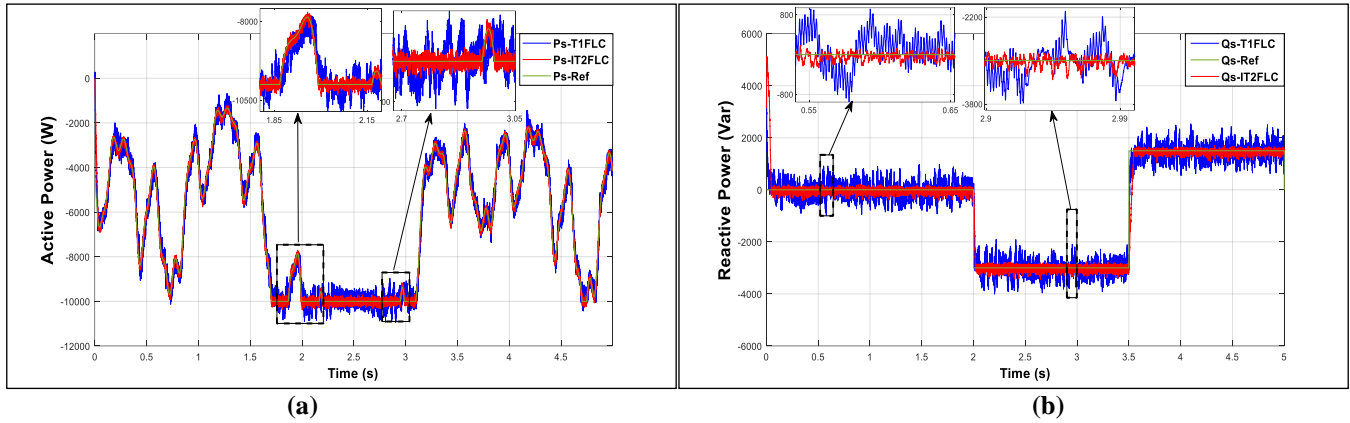


Figure 12: DFIG power (a)  $P_s$ ; (b)  $Q_s$ . Source: Authors, (2025).

The results presented in Figure 12 and Table 3 reveal distinct differences in controller behavior. The T1-FLC controller exhibited brief instances of overshoot before settling to the reference trajectory, whereas the proposed IT2-FLC maintained precise tracking without any overshoot. This performance underscores the IT2-FLC’s resilience to disturbances, variations in internal parameters, and rapid shifts in the reference input. Moreover, the IT2-FLC approach produced lower fluctuations in both  $P_s$  and  $Q_s$ , a benefit illustrated in Figure 12. Table 2 reports performance metrics and reduction ratios for each controller under changes to machine parameters, including rise time, ISE, IAE, ITSE, and ITAE. A comparison of these measures shows that the T2-FLC outperforms the T1-FLC. However, when evaluated against the energy-related criteria, the IT2-FLC delivers the best overall efficiency, as reflected by the values in Table 2. As such, the simulation results demonstrate that the IT2-FLC has superior robustness and energy performance. It has reduced power ripple and improved tracking compared to the T1-FLC examined.

Table2: Numerical results from the robustness Test.

	IAE	ITAE	ISE	ITSE	Rise Time (sec)
$P_s$ (T1-FLC)	1501	3678	7.421e05	1.63e06	0.033
$P_s$ (IT2-FLC)	434.6	938.6	2.227e05	1.008e05	0.031
Ratio	71.05%	74.48%	69.99%	93.08%	6.06%
$Q_s$ (T1-FLC)	1313	3221	6.843e05	1.563e06	0.053
$Q_s$ (IT2-FLC)	625.7	1256	6.013e05	1.253e06	0.05
Ratio	52.35%	61.01%	12.12%	19.83%	5.66%

Source: Authors, (2025).

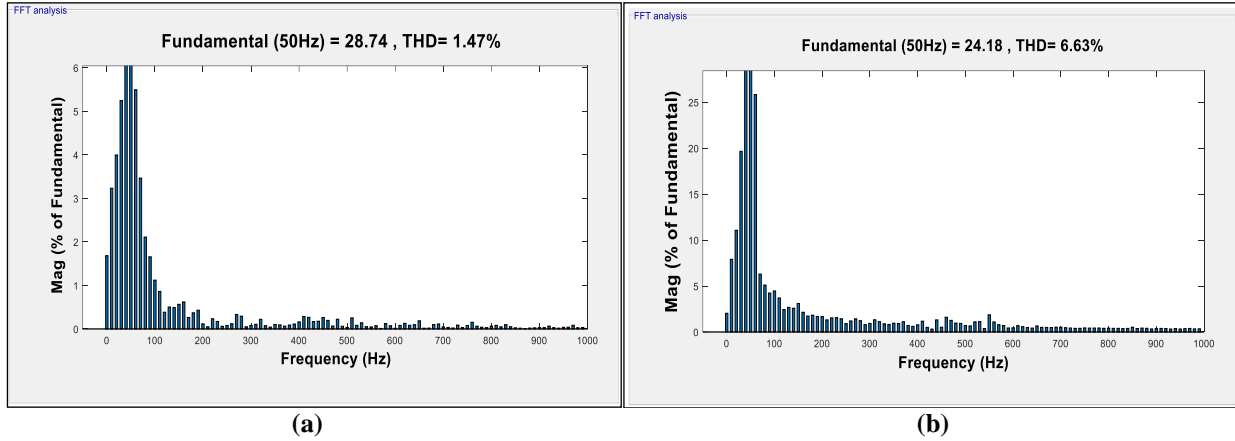


Figure 13: (a) THD IT2-FLC; THD T1-FLC. Source: Authors, (2025).

Figures 13(a) and (b) present the THD of the current under two distinct control strategies. Using the conventional T1-FLC, the current THD measured 6.63%. By contrast, the IT2-FLC reduced THD to 1.47%. This corresponds to a 77.82% decrease in current ripple when employing the IT2-FLC compared with the T1-FLC (refer to Table 3), indicating a substantial enhancement in current waveform quality. Moreover, the fundamental component (50 Hz) of the current exhibited a larger amplitude under the IT2-FLC: 28.74 A versus 24.18 A with the T1-FLC. This increase in fundamental amplitude, together with the marked THD reduction, underscores the superior performance of the proposed IT2-FLC strategy. Overall, simulation outcomes indicate that the IT2-FLC offers more robust operation in the presence of parameter variations and uncertain disturbances, making it the preferable control approach for maintaining high current quality under challenging conditions.

Table 3: The current THD values between the two tests.

	THD % (Test 1)	THD % (Test 2)
T1-FLC	1.83	1.35
IT2-FLC	6.63	1.47
Ratio	26.22%	77.82%

Source: Authors, (2025).

#### IV. CONCLUSIONS

This research develops and assesses control strategies for converting WE into electrical power by independently regulating  $P_s$  and  $Q_s$  using T1-FLC and IT2-FLC. The focus is on a model of a 10 kW doubly fed induction generator (DFIG), performing simulations under variable WS conditions, and implementing the IT2-FLC in MATLAB to enable a direct comparison with conventional T1-FLC-based control. Two stress tests evaluate system robustness: one examines the response to very high WS, and the other explores the effects of changing system parameters. Comparative results indicate that the IT2-FLC produces superior performance across the examined metrics. Quantitative measures—such as reductions in error, lower overshoot, and diminished fluctuations in both  $P_s$  and  $Q_s$  confirm its advantage. Additionally, parameter variations influenced current waveform quality, reflected in changes to total harmonic distortion (THD); however, the IT2-FLC approach mitigated these adverse effects more effectively than the conventional T1-FLC. Overall, the findings demonstrate that IT2-FLC offers improved resilience and cleaner power delivery in WECS.

#### V APPENDIX

Table 4: Parameters of the DFIG and WT.

Parameters	Value	Parameters	Value
$R_s$	0.455 $\Omega$	$P$	2
$R_r$	0.19 $\Omega$	$\rho$	1.225 Kg/m <sup>3</sup>
$L_s$	0.07 H	$R_b$ (Blade radius)	3.45m
$L_r$	0.0213 H	$H_m$ (Inertia constant)	2s
$M$	0.034 H	$D$ (Damping coefficients)	0.01 Nm.s/rad

Source: [14].

#### VI. AUTHOR'S CONTRIBUTION

- Conceptualization:** Izzeddine Allali, Abdelber Bendaoud.
- Methodology:** Izzeddine Allali, Abdelber Bendaoud.
- Investigation:** Izzeddine Allali, Abdelber Bendaoud.
- Discussion of results:** Izzeddine Allali and Abdelber Bendaoud.
- Writing – Original Draft:** Izzeddine Allali.
- Writing – Review and Editing:** Izzeddine Allali, Abdelber Bendaoud.

**Resources:** Izzeddine Allali.

**Supervision:** Abdelber Bendaoud.

**Approval of the final text:** Abdelber Bendaoud.

### III. REFERENCE

- [1] Mousavi, Y., Bevan, G., Kucukdemiral, I. B., & Fekih, A. "Sliding mode control of wind energy conversion systems: Trends and applications". *Renewable and Sustainable Energy Reviews*, vol. 167, pp. 112734, 2022. <https://doi.org/10.1016/j.rser.2022.112734>
- [2] Fridi, S. K., Koonthar, M. A., Jamali, M. I., Alaas, Z. M., Alsharif, M. H., Kim, M. K., ... & Ahmed, M. M. R. "Winds of progress: an in-depth exploration of offshore, floating, and onshore wind turbines as cornerstones for sustainable energy generation and environmental stewardship." *IEEE Access*, vol.12, pp. 66147-66166, 2024. <https://doi.org/10.1109/ACCESS.2024.3397243>
- [3] M. H. Alsharif, A. Jahid, R. Kannadasan, and M.-K. Kim, "Unleashing the potential of sixth generation (6G) wireless networks in smart energy grid management: A comprehensive review," *Energy Rep.*, vol. 11, pp. 1376–1398, Jun. 2024. <https://doi.org/10.1016/j.egy.2024.01.011>
- [4] Jaiswal, K. K., Chowdhury, C. R., Yadav, D., Verma, R., Dutta, S., Jaiswal, K. S., & Karuppasamy, K. S. K., "Renewable and sustainable clean energy development and impact on social, economic, and environmental health". *Energy nexus*, vol. 7, pp.100118, 2022. <https://doi.org/10.1016/j.nexus.2022.100118>
- [5] GWEC. Global Wind Report 2024. Global Wind Energy Council. (2024).
- [6] Benbouhenni, H., Bizon, N., Mosaad, M. I., Colak, I., Djilali, A. B., & Gasmi, H, "Enhancement of the power quality of DFIG-based dual-rotor wind turbine systems using fractional order fuzzy controller", *Expert Systems with Applications*, vol. 238, pp. 121695, 2024. <https://doi.org/10.1016/j.eswa.2023.121695>
- [7] HERIZI, Abdelghafour et ROUABHI, Riyadh. "Hybrid Control Using Sliding Mode Control with Interval Type-2 Fuzzy Controller of a Doubly Fed Induction Generator for Wind Energy Conversion". *International Journal of Intelligent Engineering & Systems*, vol.15, no.1, pp.549-562, 2022. <https://doi.org/10.22266/ijies2022.0228.50>
- [8] Itouchene, H., Amrane, F., Boudries, Z., Mekhilef, S., Benbouhenni, H., & Bizon, N. "Enhancing the performance of grid-connected DFIG systems using prescribed convergence law". *Scientific Reports*, vol.15, no.1, pp.28550, 2025. <https://doi.org/10.1038/s41598-025-13847-x>.
- [9] HEMEYINE, Ahmed Vall, ABOU, Ahmed, TIDJANI, Naoual, et al. "Robust takagi sugeno fuzzy models control for a variable speed wind turbine based a DFI-generator". *International Journal of Intelligent Engineering and Systems*, vol.13, no 3, pp. 90-100,2020. <https://doi.org/10.22266/ijies2020.0630.09>
- [10] Tang, H. H., & Ahmed, N. S. "Fuzzy logic approach for controlling uncertainties and nonlinear systems: a comprehensive review of applications and advances". *Systems Science & Control Engineering*, vol. 12,no.1, pp. 2394429,2024.<https://doi.org/10.1080/21642583.2024.2394429>
- [11] NISHANTH, F. Paul, DASH, Saroj Kumar, et MAHAPATRO, Soumya Ranjan. "Critical study of type-2 fuzzy logic control from theory to applications: A state-of-the-art comprehensive survey. e-Prime-Advances in Electrical Engineering", *Electronics and Energy*, vol. 10, p. 100771,2024. <https://doi.org/10.1016/j.prime.2024.100771>
- [12] Abbas, A. K., Al Mashhadany, Y., Hameed, M. J., & Algburi, S. "Review of intelligent control systems with robotics". *Indonesian Journal of Electrical Engineering and Informatics (IJEEI)*, vol.10, no.4, pp.734-753,2022. <https://doi.org/10.52549/ijeei.v10i4.3628>
- [13] Yan, S. R., Dai, Y., Shakibjoo, A. D., Zhu, L., Taghizadeh, S., Ghaderpour, E., & Mohammadzadeh, A., " A fractional-order multiple-model type-2 fuzzy control for interconnected power systems incorporating renewable energies and demand response", *Energy Reports*, vol.12, pp. 187-196,2024. <https://doi.org/10.1016/j.egy.2024.06.018>
- [14] I. Allali, B.Dehiba, "A Comparative Study of Interval Type-2 and Type-1 Fuzzy Sliding Mode in Controlling DFIG-Based Wind Energy Conversion System", *Nigerian Journal of Technological Development*, vol.22, no.3, pp.101.110, 2025. <http://dx.doi.org/10.63746/njtd.v22i3.2818>.
- [15] KADDACHE, M., DRID, S., KHEMIS, A., et al. "Maximum power point tracking improvement using type-2 fuzzy controller for wind system based on the double fed induction generator. *Electrical Engineering & Electromechanics*", no 2, pp. 61-66, 2024. <https://doi.org/10.20998/2074-272X.2024.2.09>
- [16] HAMDAN, I., YOUSSEF, Marwa MM, et NOURELDEEN, Omar. " Influence of interval type-2 fuzzy control approach for a grid-interconnected doubly-fed induction generator driven by wind energy turbines in variable-speed system". *SN Applied Sciences*, vol. 5, no. 1, pp. 25,2023. <https://doi.org/10.1007/s42452-022-05242-2>
- [17] VILLANUEVA, Iván, PONCE, Pedro, et MOLINA, Arturo. " Interval type 2 fuzzy logic controller for rotor voltage of a doubly-fed induction generator and pitch angle of wind turbine blades". *IFAC-PapersOnLine*, vol. 48, no 3, p. 2195-2202,2015. <https://doi.org/10.1016/j.ifacol.2015.06.414>
- [18] MORADI, Hassan, ALINEJAD-BEROMI, Yousef, YAGHOBI, Hamid, et al. "Sliding mode type-2 neuro-fuzzy power control of grid-connected DFIG for wind energy conversion system". *IET Renewable Power Generation*, vol. 13, no 13, p. 2435-2442, 2019. <https://doi.org/10.1049/iet-rpg.2019.0066>
- [19] KOUADRIA, Mohamed Abdeldjabbar, KOUADRIA, Selman, et BOUZID, Mohamed Amine. " Type-2 Fuzzy Control of DFIG for Wind Energy Conversion Systems". *ITEGAM-JETIA*, vol. 11, no 53, p. 154-161,2025. DOI: <https://doi.org/10.5935/jetia.v11i53.1640>
- [20] ELMOUHI, Nouredine, ESSADKI, Ahmed, et ELAIMANI, Hind. " Robust control of wind turbine based on doubly-fed induction generator optimized by genetic algorithm". *International Journal of Power Electronics and Drive Systems (IJPEDS)*, vol. 13, no 2, p. 674-688,2022. <https://doi.org/10.11591/ijped.v13.i2.pp674-688>
- [21] Carpintero-Renteria, M., Santos-Martin, D., Lent, A., & Ramos, C, "Wind turbine power coefficient models based on neural networks and polynomial fitting", *IET Renewable Power Generation*, vol.14, no. 11, pp. 1841-1849, 2020. <https://doi.org/10.1049/iet-rpg.2019.1162>
- [22] Castillo, OC, Andrade, VR, Rivas, JJR, & González, RO., "Comparison of power coefficients in wind turbines considering the tip speed ratio and blade pitch angle", *Energies*, vol.16, no.6,pp2774, 2023.<https://doi.org/10.3390/en16062774>
- [23] Oualah, O., Kerdoun, D., et Boumassata, A." Super-twisting sliding mode control for brushless doubly fed reluctance generator based on wind energy conversion system". *Electrical Engineering & Electromechanics*, vol.2, pp. 86-92, 2023. <https://doi.org/10.20998/2074-272X.2023.2.13>
- [24] Mousa, H. H., Youssef, A. R., & Mohamed, E. E. "Hybrid and adaptive sectors P&O MPPT algorithm based wind generation system". *Renewable Energy*, vol.145, pp. 1412-1429,2020. <https://doi.org/10.1016/j.renene.2019.06.078>

- [25] Kadri, A., Marzougui, H., Aouiti, A., & Bacha, F., "Energy management and control strategy for a DFIG wind turbine/fuel cell hybrid system with super capacitor storage system", *Energy*, vol. 192, pp 116518, 2020. <https://doi.org/10.1016/j.energy.2019.116518>
- [26] Gambier, A. "Pitch control of three bladed large wind energy converters—a review. *Energies*", vol.14, no.23, pp.8083,2021, <https://doi.org/10.3390/en14238083>
- [27] Akhbari, A.; Rahimi, M. "Control and stability analysis of DFIG wind system at the load following mode in a DC microgridcomprising wind and micro turbine sources and constant power loads". *Int. J. Electr. Power Energy Syst.* vol.117, pp.105622,2020. <https://doi.org/10.1016/j.ijepes.2019.105622>
- [28] Belachew, D.; Gebeyehu, D.; Tamrat, B. "Evaluating the performances of PI controller (2DOF) under linear and nonlinear operations of DFIG-based WECS". *Heliyon* , 2022, vol. 8, no 12,2022.<https://doi.org/10.1016/j.heliyon.2022.e11912>
- [29] Chakib, M., Nasser, T., & Essadki, A. "Comparative study of active disturbance rejection control with RST control for variable wind speed turbine based on doubly fed induction generator connected to the grid". *International Journal of Intelligent Engineering and Systems*, vol. 13,no.1, pp. 248- 258,2020. <https://doi.org/10.22266/ijies2020.0229.23>
- [30] D. Hidalgo, O. Castillo, P. Melin, "Type-1 and type-2 fuzzy inference systems as integration methods in modular neural networks for multimodal biometry and its optimization with genetic algorithms", *Inf Sci (Ny)*, vol.179, no.13, pp. 2123–2145,2009. <https://doi.org/10.1016/j.ins.2008.07.013>
- [31] Narthana, S., & Gnanavadivel, J, "Power quality analysis of interleaved Cuk configuration-based interval type-2 fuzzy logic controller for battery charging in electric vehicles", *Arabian Journal for Science and Engineering*, Vol. 49, no.5, pp. 6259-6273, 2024. <https://doi.org/10.1007/s13369-023-08189-7>
- [32] Wu, D., & Mendel, J. M. "Recommendations on designing practical interval type-2 fuzzy systems". *Engineering Applications of Artificial Intelligence*, vol.85, pp. 182-193, 2019.<https://doi.org/10.1016/j.engappai.2019.06.012>